

Table S1. Primer sequences

Name	Forward Primer	Reverse Primer
ChIP primers		
Ctrl	AACCTGCAAAACATGGTTATTT	AATTTGCCCAAACAGCAAGT
B1	GTTGGGAAATGGTGGATGAC	GTGACCCAAGCGATGAGTTT
B2	GAGGGAGGGAGTAAGGGA	ACTCGAAGCCTTTTCCAGGT
B3	AAGGGCTGAGTGTGGATGGA	CAGGGCACCAGAAAAAGCAG
R1	CTTGACGGTCTGGATGTGGT	AGGAGCTGCTCAATGGGAAC
R2	GTTCCCATTGAGCAGCTCCT	AGAGCAACAGGTGACCCAAG
C1	GCCTTGGGACTTGAGGACTT	TTACCACATCCAGACCGTCA
C2	TTCTCCATGAGGTCTGTGAGG	GCCTGGTGTGTACCACCTTC
qPCR primers		
TCF7	CTGGCTTCTACTCCCTGACCT	ACCAGAACCTAGCATCAAGGA
LEF1	AGAACACCCCGATGACGGA	GGCATCATTATGTACCCGGAAT
BCL6	GTTGTGGACACTTGCCGGAA	CTCTTCACGAGGAGGCTTGAT
PRDM1	AACTTCTTGTGTGGTATTGTCGG	CAGTGCTCGGTTGCTTTAGAC
RUNX3	GCGAGGGAAGAGTTTCACCC	TTGATGGCTCGGTGGTAGGT
ACTB	ATGGCCACGGCTGCTTCCAGC	CATGGTGGTGCCGCCAGACAG

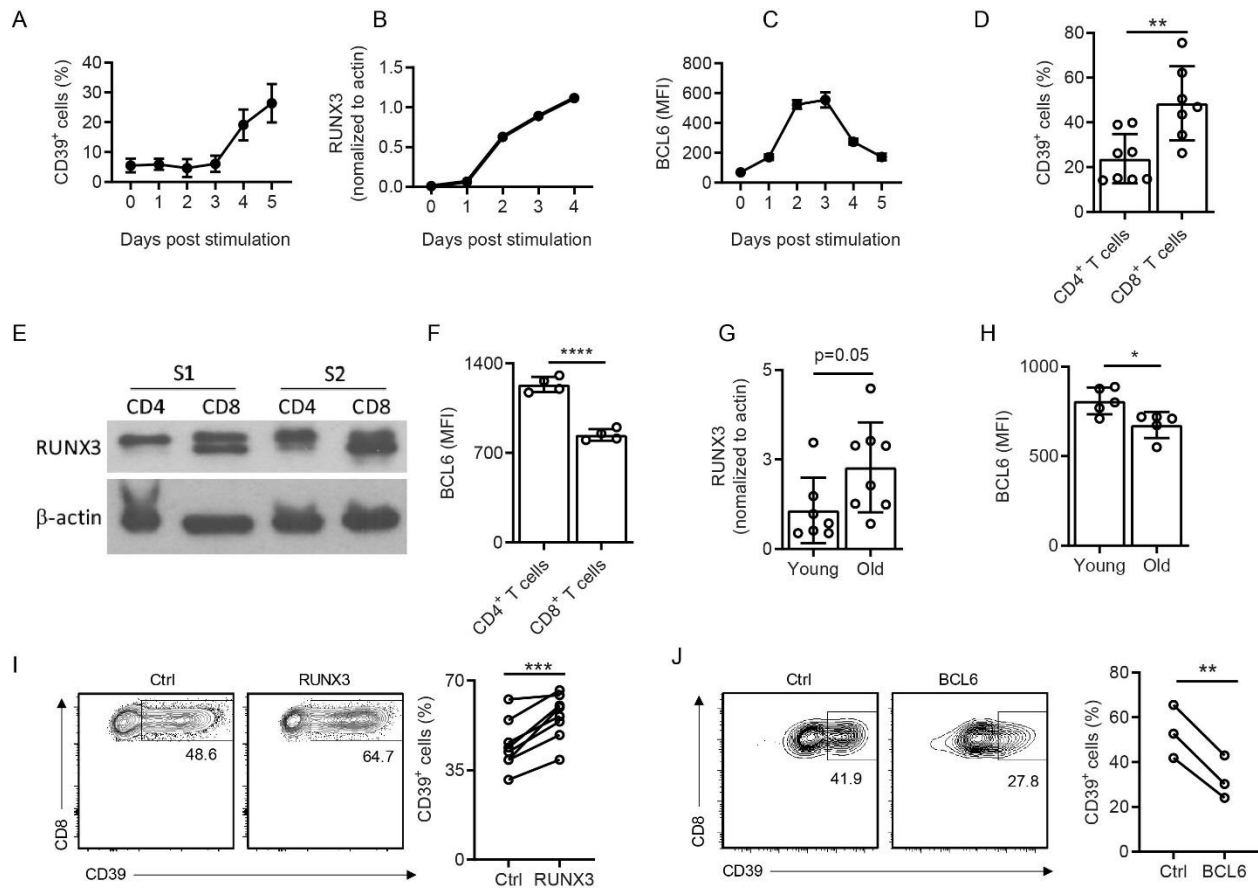


Figure S1, related to Figure 2. Transcriptional regulation of *ENTPD1* by RUNX3 and BCL6.

(A-C) Purified human naïve CD4 cells were activated with anti-CD3/CD28 Dynabeads for indicated times; CD39 expression (A) and BCL6 expression (C) were assessed by flow cytometry; RUNX3 protein expression (B) by immunoblot. (D-E) Human total T cells from PBMC were activated with anti-CD3/CD28 Dynabeads for 4 days; CD39 expression on CD4 or CD8 T cells was detected by flow cytometry (D). RUNX3 protein was quantified by immunoblot on purified activated CD4 and CD8 T cells. (F) Human CD4 or CD8 T cells were activated with anti-CD3/CD28 Dynabeads for 3 days, BCL6 expression was determined by flow cytometry. (G, H) Naïve CD4 T cells from young and old individuals were activated with anti-CD3/CD28 Dynabeads for 4 (G) or 3 days (H). RUNX3 and BCL6 protein were examined by immunoblot or flow cytometry. (I, J) RUNX3 and BCL6 were overexpressed in CD8 T cells and CD39 expression was determined as described in Figures 2A and C for CD4 T cells. Data are shown as mean \pm SEM; comparisons

by two-tailed paired t -test (D, F, I, J) or by two-tailed unpaired t -test (G, H). * $P < 0.05$, ** $P \leq 0.01$,
*** $P \leq 0.001$.

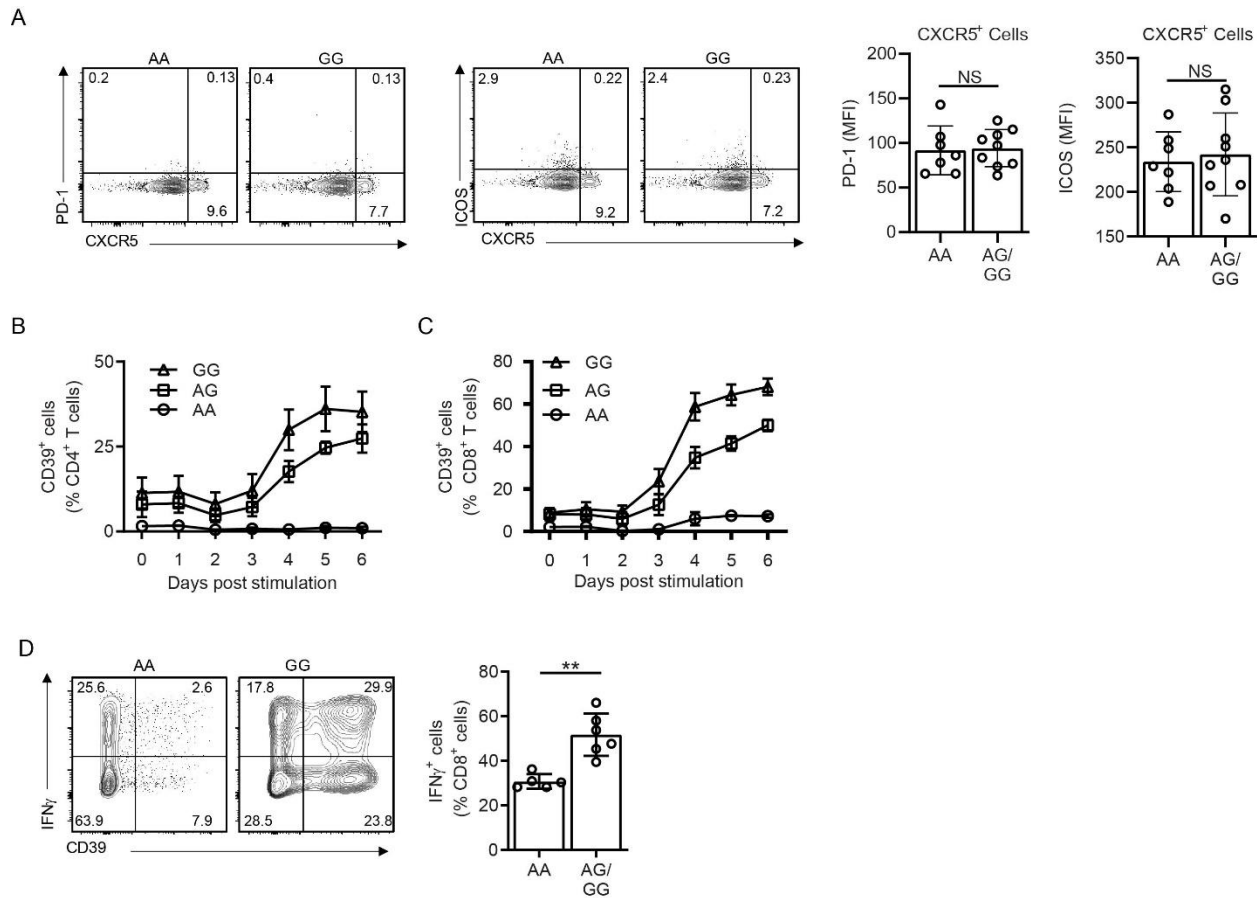


Figure S2, related to Figure 3. Influence of *ENTPD1* SNP on T cell differentiation.

(A) PD-1 and ICOS expression on circulating Tfh cells. (B, C) Total T cells carrying the indicated *ENTPD1* promoter SNP were activated with anti-CD3/CD28 Dynabeads; CD39 expression on CD4 (B) and CD8 (C) at indicated time points was assessed by flow cytometry. (D) IFN γ production after ionomycin/PMA stimulation of CD8⁺ T cells carrying the AA or AG/GG SNP as described in Figure 3D for CD4 T cells. Data are shown as mean \pm SEM, comparison by two-tailed unpaired *t*-test. ***P* < 0.01, NS, not significant.

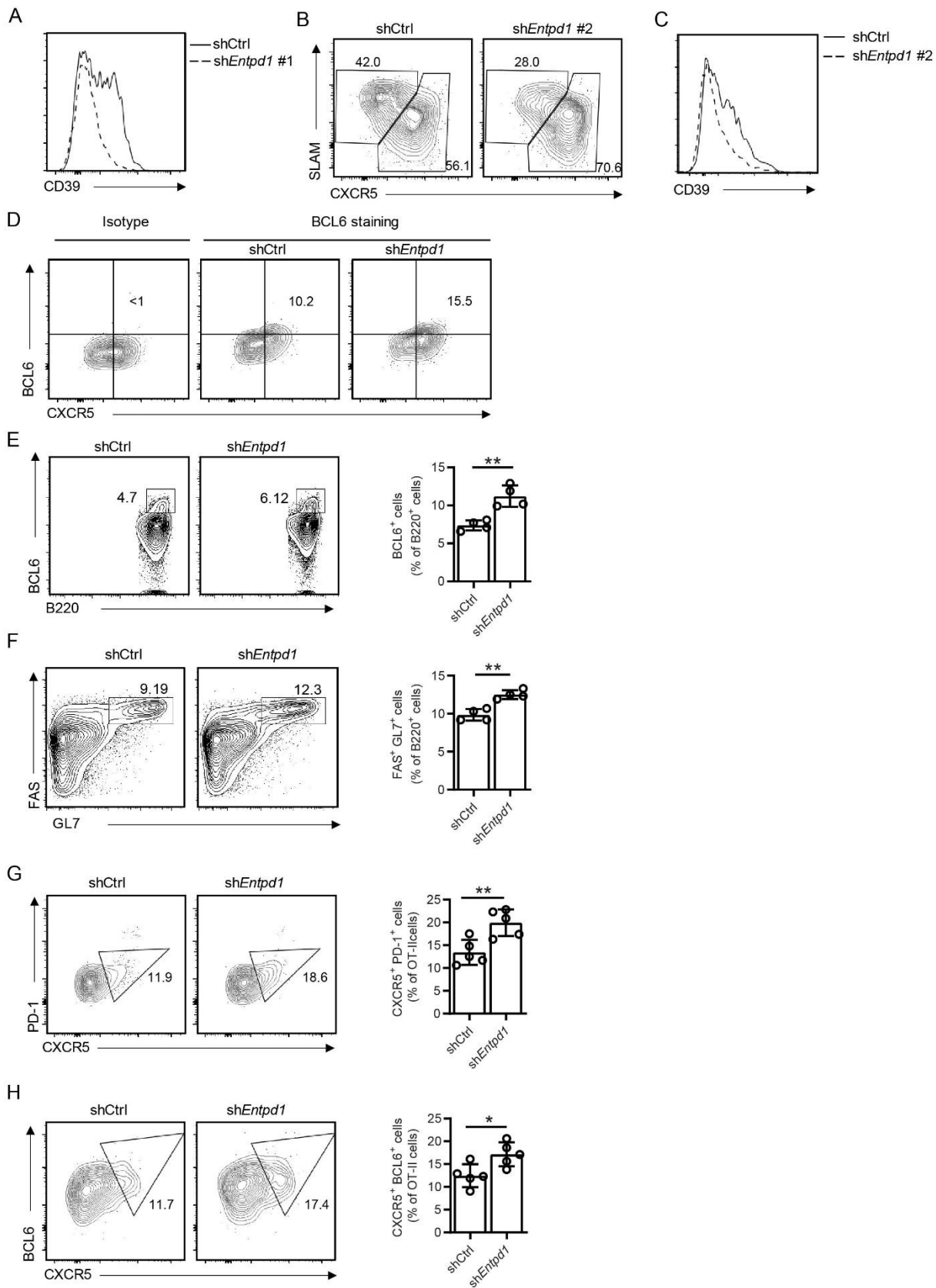
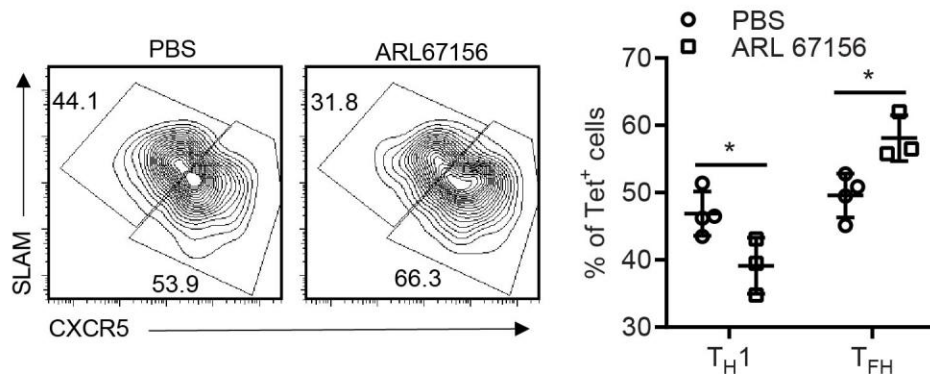
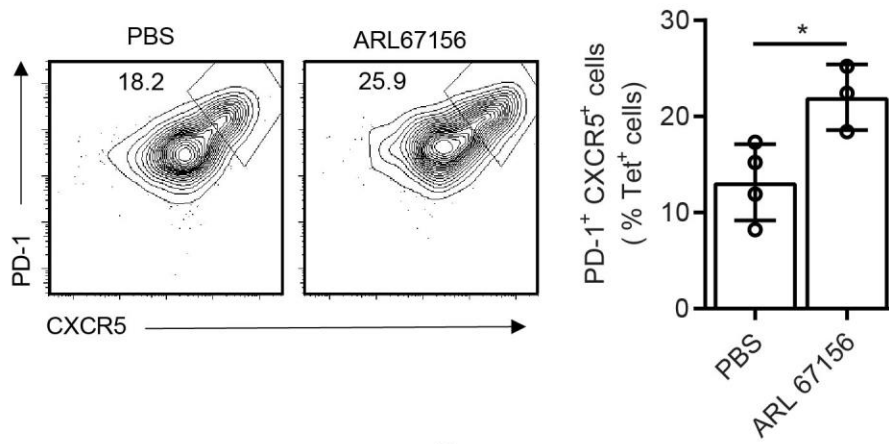


Figure S3, related to Figure 4. Effect of *Entpd1* silencing on murine T cell responses after LCMV infection or NP-OVA immunization. (A) Efficacy of sh*Entpd1* #1, as used in Figure 4A-C, in silencing *Entpd1* in SMARTA T cells. (B, C) Experiments as shown in Fig. 4 A-C were repeated with using sh*Entpd1* #2 to silence CD39 expression in SMARTA cells. Data are from one experiment, 4 mice in each group. (D) Expression of BCL6 after *Entpd1* silencing in SMARTA cells, replicate experiment from Figure 4C with isotype control. (E-F) Analysis of B cell responses after LCMV infection from experiments shown in Figures 4A-C. (G-H) Analysis of Tfh responses after NP-OVA immunization as shown in Figures 4E-H. Data were compared by two-tailed unpaired *t*-test. * $P < 0.05$, ** $P \leq 0.01$.

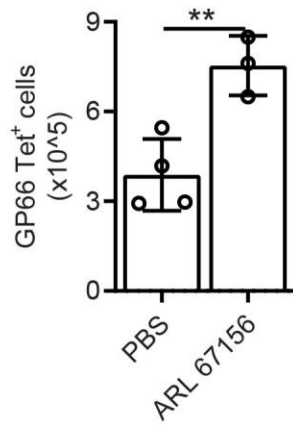
A



B



C



D

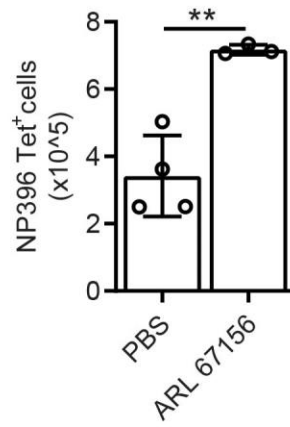


Figure S4, related to Figure 4. Effect of CD39 inhibition on CD4 T cell differentiation in mice after LCMV infection. B6 mice infected with LCMV received intraperitoneal injection of PBS or the CD39 inhibitor ARL 67156 every other day; splenocytes were analyzed after 8 (A-B) and 28 days (C-D). Representative contour plots of the expression of SLAM (A) and PD-1^{high} (B) in CXCR5⁺ GP66-77 IA^b tetramer⁺ CD4 T cells (left). Frequencies of splenic CXCR5^{high} SLAM^{low} (Tfh) and CXCR5^{low}SLAM^{high} (T_H1) CD4 T cells (A) and PD-1^{high} CXCR5⁺ GC Tfh (B) with 3-4 mice in each group are shown as mean±SEM (right). Number of GP66-77 IA^b tetramer⁺ CD4 (C) and of NP396-404 H2D^b CD8 T cells (D) with 3-4 mice in each group are represented as mean±SEM. Data were compared by two-tailed unpaired *t*-test. *P*<0.05, ***P*≤0.01.

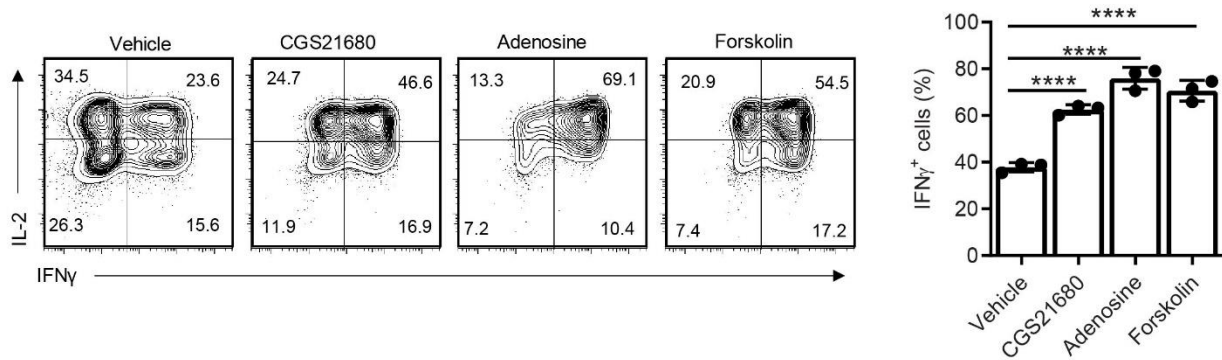


Figure S5, related to Figure 5. Adenosine 2A receptor (A2AR) signaling enhances T_H1 differentiation of human naïve CD4 T cells. Human naïve CD4 were cultured under TH1 condition in the presence of the A2AR agonist CGS21680, adenosine and forskolin, respectively for 5 days; IL-2 and IFN γ production were analyzed by flow cytometry after restimulation with PMA plus ionomycin for 3 h. Representative contour plots and data from three experiments are shown. Data are shown as mean \pm SEM and were compared by one-way ANOVA. **** $P\leq 0.0001$.

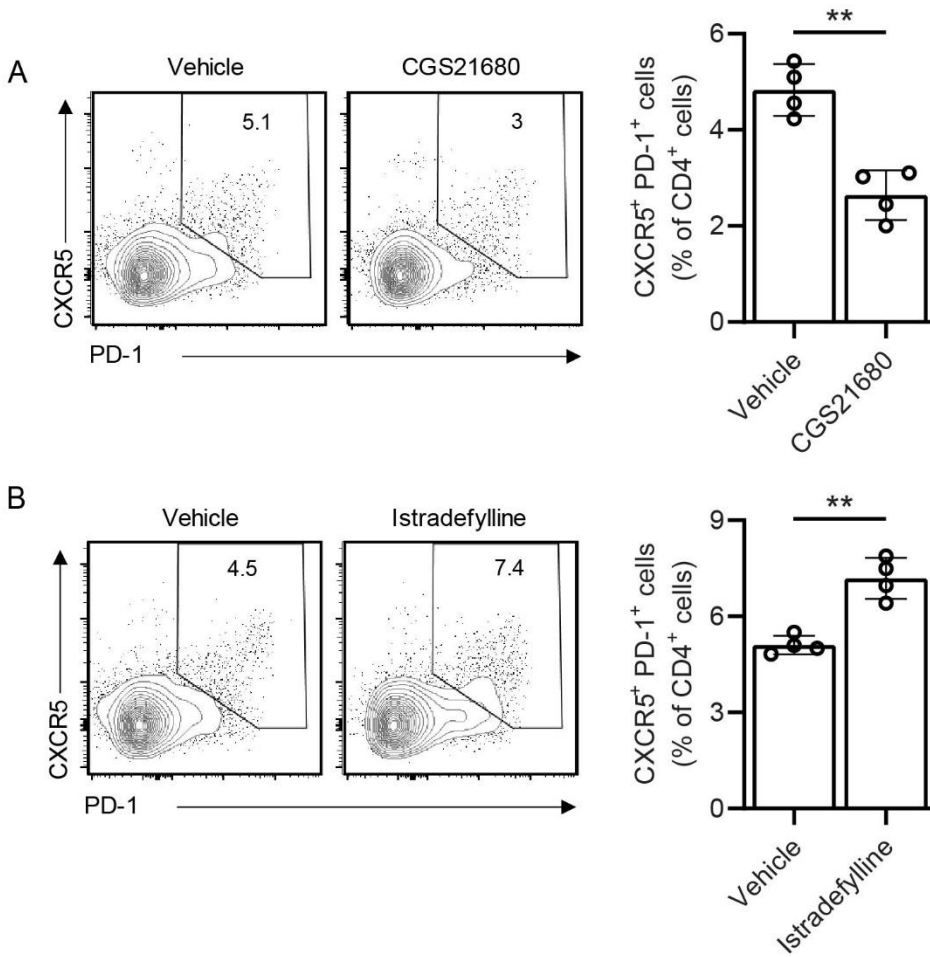


Figure S6, related to Figure 6. Effect of adenosine 2A receptor (A2AR) signaling on T cell differentiation in mice after NP-OVA immunization. Wild-type mice immunized with NP-OVA were treated with CGS21680 (A) or istradefylline (B). Tfh cell frequencies were obtained on day 12 by flow cytometry. Data are shown as mean \pm SEM and were compared by two-tailed unpaired *t*-test. ** $P\leq 0.01$.

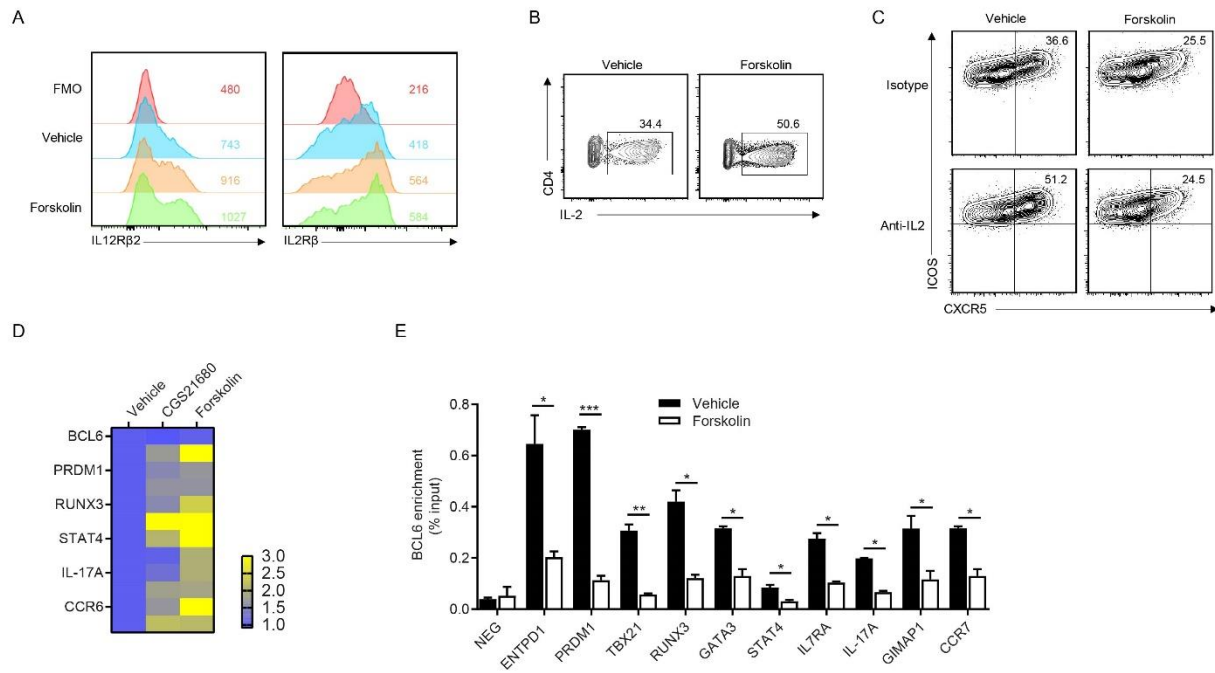


Figure S7, related to Figure 7. Effect of adenosine 2A receptor (A_{2A}R) signaling on human

T_H1 and Tfh differentiation. (A) Human naïve CD4 were activated by anti-CD3/CD28

Dynabeads under T_H1-polarizing condition for 48 h in the presence of vehicle control, CGS21680 or forskolin; IL-12Rβ (left) or IL-2Rβ (right) expression were analyzed by flow cytometry.

(B) Human naïve CD4 were cultured under Tfh condition, forskolin was added on day 1 of culture; IL-2 production was determined by flow cytometry on day 5 after PMA/ionomycin re-stimulation for 3 h. Contour plot is representative of 3 experiments.

(C) Human naïve CD4 were cultured under Tfh condition with vehicle or forskolin in the presence or absence of anti-IL2 antibodies for 5 days; cells were analyzed by flow cytometry for ICOS and CXCR5 expression. Data are representative of three experiments.

(D) Expression BCL6 target gene transcripts by naïve CD4 T cells activated under Tfh condition for 3 days in the presence or absence of CGS21689 or forskolin. Data are shown as mean fold difference of triplicates of treated

compared to control samples. (E) ChIP-PCR for BCL6 enrichment at indicated BCL6 target

genes in naïve CD4 T cell activated in the presence or absence of forskolin under Tfh polarizing conditions for 3 days. Results are shown as mean \pm SEM of three experiments and compared by multiple *t*-test. * P <0.05, ** P ≤0.01, *** P ≤0.001.

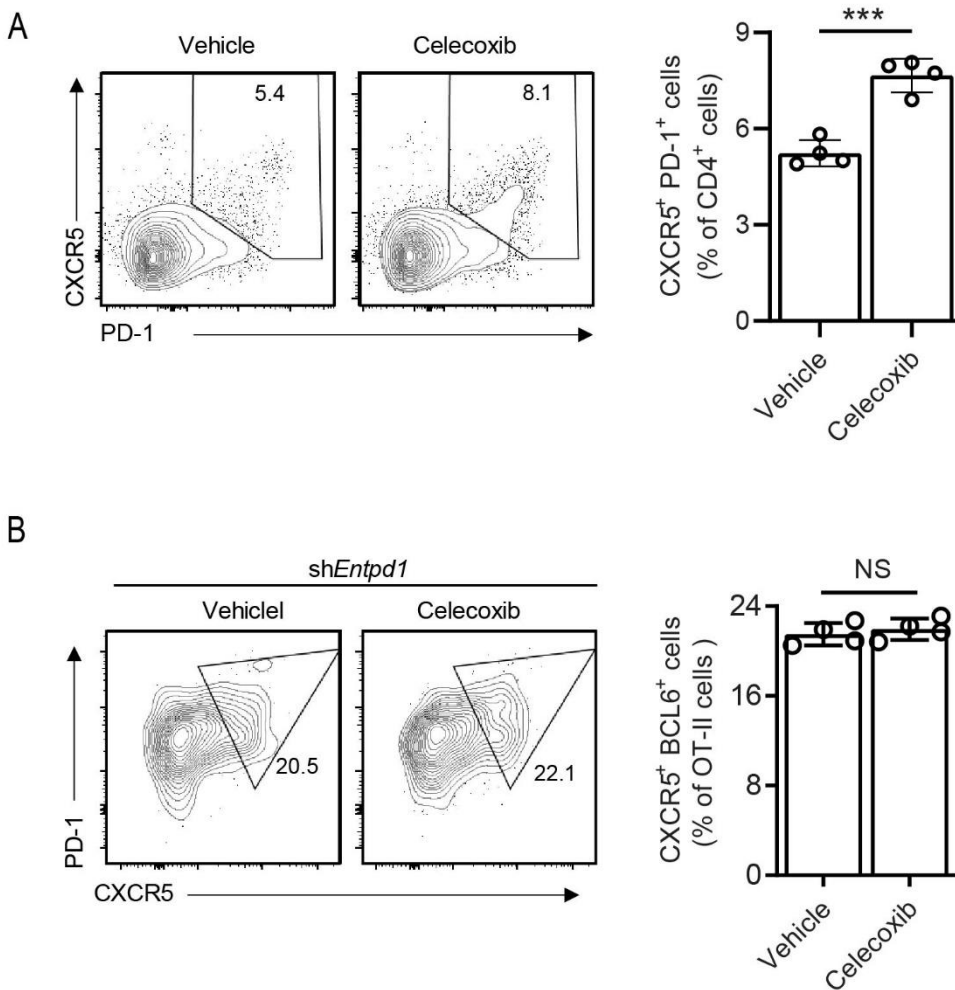


Figure S8, related to Figure 8. COX-2 inhibition enhances Tfh differentiation through repressing CD39. A. B6 mice were immunized with NP-OVA and treated with Celecoxib as described in Figure 8D. Tfh frequencies were determined on day 12. B. OT-II CD4⁺ T cells were transduced and adoptively transferred and reconstituted mice were immunized and treated as described in Figure 8G. Tfh frequencies were determined on day 12 after immunization. Data are shown as mean \pm SEM and were compared by two-tailed unpaired *t*-test. *** $P \leq 0.001$. NS, not significant.